Journal of Clinical Monitoring and Computing
https://doi.org/10.1007/s10877-018-00245-0

ORIGINAL RESEARCH

Near-real-time pulmonary shunt and dead space measurement with micropore membrane inlet mass spectrometry in pigs with induced pulmonary embolism or acute lung failure

D. Gerber[1] · R. Vasireddy[1] · B. Varadarajan[1] · V. Hartwich[1] · M. Y. Schär[1] · B. Eberle[1] · A. Vogt[1]

Received: 4 September 2018 / Accepted: 22 December 2018
© Springer Nature B.V. 2019

Abstract
The multiple inert gas elimination technique (MIGET) using gas chromatography (GC) is an established but time-consuming method of determining ventilation/perfusion (VA/Q) distributions. MIGET—when performed using Micropore Membrane Inlet Mass Spectrometry (MMIMS)—has been proven to correlate well with GC-MIGET and reduces analysis time substantially. We aimed at comparing shunt fractions and dead space derived from MMIMS–MIGET with Riley shunt and Bohr dead space, respectively. Thirty anesthetized pigs were randomly assigned to lavage or pulmonary embolism groups. Inert gas infusion (saline mixture of SF6, krypton, desflurane, enflurane, diethyl ether, acetone) was maintained, and after induction of lung damage, blood and breath samples were taken at 15-min intervals over 4 h. The samples were injected into the MMIMS, and resultant retention and excretion data were translated to VA/Q distributions. We compared MMIMS-derived shunt (MM-S) to Riley shunt, and MMIMS-derived dead space (MM-VD) to Bohr dead space in 349 data pairs. MM-S was on average lower than Riley shunt (-0.05 ± 0.10), with lower and upper limits of agreement of -0.15 and 0.04, respectively. MM-VD was on average lower than Bohr dead space (-0.09 ± 0.14), with lower and upper limits of agreement of -0.24 and 0.05. MM-S and MM-VD correlated and agreed well with Riley shunt and with Bohr dead space. MM-S increased significantly after lung injury only in the lavage group, whereas MM-VD increased significantly in both groups. This is the first work evaluating and demonstrating the feasibility of near real-time VA/Q distribution measurements with the MIGET and the MMIMS methods.

Keywords Pulmonary embolism · Intrapulmonary shunt and O_2 therapy · Respiratory function: dead space · VQ mismatch: causes · Level of hypoxemia: factors impacting

1 Introduction

Finding an optimal approach for therapy of acute respiratory failure in a clinical scenario remains a challenge. Such therapy is essential for supporting an injured lung until the basic lung injury resolves. Effectual respiratory support must be provided, taking into account the pathophysiology responsible for the altered pulmonary gas exchange. During and after anesthesia or even sedation, hypoxemia is still a common complication. Postoperative pulmonary complications are reported in 3–10% of elective abdominal surgeries and emergency operations [1]. In a UK study, major complications were reported in 32% of thoracic surgeries [2]. Although applied research has resulted in significantly lower mortality rates for patients with acute lung injury or acute respiratory distress syndrome (a decrease of approximately 1.1% per year between 1994 and 2006), pooled overall mortality remains at 43% for studies published between 1994 and 2006 [3].

Normal pulmonary gas exchange depends on physiological matching of alveolar ventilation and pulmonary capillary perfusion [4]. Therefore, precise knowledge of the mechanisms of arterial hypoxemia is necessary. The major causes of hypoxemia are hypoventilation, diffusion impairment

Electronic supplementary material The online version of this article (https://doi.org/10.1007/s10877-018-00245-0) contains supplementary material, which is available to authorized users.

✉ A. Vogt
andreas.vogt@insel.ch

[1] Department of Anaesthesiology and Pain Medicine, Inselspital, Bern University Hospital, University of Bern, 3010 Bern, Switzerland

Published online: 02 January 2019

(e.g., due to dead space), ventilation/perfusion (V*A*/Q) inequality, and right-to-left shunt [5]. How these four conditions contribute to oxygenation failure is quite difficult to differentiate in a clinical scenario. Additionally, extrapulmonary factors (e.g., oxygen consumption, temperature) may also influence arterial PO_2.

Various strategies [6, 7] have been proposed to allow bedside estimation of V/Q mismatch, shunt and deadspace. The multiple inert gas elimination technique (MIGET) [8] enables the analysis of each of these four causes of hypoxemia and is therefore the most comprehensive approach for identifying the pathophysiological mechanisms which lead to blood gas alterations. After infusion of an inert gas solution through a peripheral vein, arterial, mixed-venous, and mixed-expired inert gas concentrations are measured. These measurements are subsequently used to derive retention and excretion values for each infused inert gas. Parallel to these measurements, a computer algorithm generates a standard V_A/Q distribution and calculates retention as well as excretion values for this generated standard distribution. Finally, the parameters of the standard V_A/Q distribution are altered in an iterative fashion to arrive at a V_A/Q distribution that provides the closest correlation between the calculated and measured retention as well as excretion values.

Even though MIGET has become an established method of determining V*A*/Q mismatch, the laborious and time-consuming gas chromatography (GC) used for inert gas analysis and its potential for technical errors have prevented widespread adoption of GC-MIGET in clinical practice [9, 10]. To overcome the challenges associated with standard GC-MIGET, micropore membrane inlet mass spectrometry (MMIMS) was introduced [9]. Recently MIGET by MMIMS was compared with GC-MIGET and proven to correlate well [11]. Riley shunt and volumetric capnography are frequently used to quantify alterations in intrapulmonary shunt and dead space. Riley shunt is calculated from arterial, mixed venous, and assumed pulmonary end capillary blood gas data, and dead space is evaluated based on the volumetric capnography parameters according to Bohr [10, 12, 13]. MMIMS-MIGET shunt calculated from MMIMS fitted with a single-pore probe has shown good correlation with Riley shunt in a porcine lavage lung injury model [10]. Conventional GC-MIGET has been used in several animal models to study the mechanisms of impaired pulmonary gas exchange [10, 14, 15].

In the present study, two commonly used lung injury models were employed: (i) repeated lung lavages leading to surfactant depletion, increased shunt and low V*A*/Q (lavage group), and (ii) injection of autologous clots to produce dead space and high V*A*/Q in the lung compartments (pulmonary embolism group). The aims of the study were: (i) to compare shunt fraction and dead space derived from MMIMS-MIGET with Riley shunt and Bohr dead space, and (ii) to test the temporal resolution under near-clinical conditions. We hypothesized that MMIMS-derived shunt and MMIMS-derived dead space would correlate with Riley shunt and Bohr dead space, and the raw data would be available with a delay comparable to conventional blood gas analysis.

2 Materials and methods

2.1 Instrumentation and general preparation

With approval (BE15/11) from the state animal care committee, 30 anesthetised pigs (30.6 ± 1.90 kg, mean ± SD) were enrolled in this study, which was carried out in the ESI (Experimental Surgery Unit of the medical faculty of the University of Bern, Switzerland) and in the Department of Anaesthesiology, Inselspital, Bern University Hospital, University of Bern, Switzerland. After premedication (xylazine 2 mg/kg IM, ketamine 20 mg/kg IM and atropine 0.05 mg/kg IM), anesthesia was induced by propofol 3 mg/kg IV and fentanyl 7–10 mcg/kg IV.

All animals were positioned supine. Anesthesia was maintained with a continuous infusion of propofol 6–8 mg/kg/h and fentanyl 7–10 mcg/kg/h. The airway was secured by endotracheal intubation (cuffed tracheal tube; Ruesch, Kernen, Germany). Relaxation was ensured with continuous infusion of pancuronium (first 8 pigs) or a bolus of esmeron (as the stock of pancuronium ran out). Pigs were ventilated with a SERVO-I respirator (Maquet, Rastatt, Germany) in IPPV mode. Respiratory rate was adjusted to allow initial normocapnia (tidal volume 6–8 ml/kg, PEEP 5 cm H_2O, I:E 1:2). A recruitment maneuver with tidal volumes up to 800 ml and a RR of 8/min was performed for 10 respiratory cycles prior to baseline measurements.

For hemodynamic monitoring, arterial and venous catheters were inserted via femoral and cervical cutdown. Data was recorded with a Datex-Engström monitor. A balloon-tipped flow-directed pulmonary artery catheter was introduced into the pulmonary artery for measurement of intermittent cardiac output by thermodilution (Baxter Healthcare, Deerfield, IL, USA), pulmonary artery pressures, pulmonary artery occlusion pressure, and mixed venous blood sampling. For cardiac output determination, the mean of three thermodilution measurements was used. Typical pressure waveforms obtained by pressure tracings were used to verify the position of all catheters. The mid-chest level was chosen as reference for all intravascular pressures. Flows, airway pressures and volumes were recorded by a sample out tube connector (Capnomac Ultima Ult-V Multifunctional Respiratory Monitor, Datex Ohmeda, Helsinki, Finland).

Rectal temperature was maintained between 37.5 and 39.5 °C with either heating mats or ventilators as needed. At the end of each experiment, general anesthesia was deepened

and the animals were euthanized with a central venous injection of 20 mmol potassium chloride.

2.2 Experimental protocols

Pigs were randomly assigned to lavage (LAV) or pulmonary embolism (PE) with a computer-generated randomization table. In the lavage group, alveolar damage was induced by surfactant washout as described in previous studies [10]. In short, the lung was repeatedly lavaged with 30 ml/kg warmed Ringer's lactate over the cuffed tracheal tube until the oxygenation index was below $PaO_2/FIO_2 < 200$, representing acute lung failure (shift of ventilation-perfusion distribution to low V*A*/Q values and shunt due to alveolar collapse and alveolar flooding). In the pulmonary embolism group, lung damage was induced through injection of autologous blood clots via a large-bore catheter (Arrow 9 Fr. Multi Access Catheter) into the inferior vena cava (modified after [16]). This led to a partially reversible obstruction of lung perfusion and shift of V*A*/Q distribution to high V*A*/Q values and dead space. A 200 ml bolus of Ringer's lactate was used for hemodynamic support after induction of lung injury. Noradrenaline or adrenaline was used if mean arterial blood pressure was below 55 mmHg after this bolus.

After instrumentation a null sample was taken to ensure absence of inert gases in the animal and connected tubing before the beginning of the inert gas infusion. This null sample will be referred to as T1 hereafter. Infusion of inert gas solution was started at a rate of 240 ml/h using a volumetric infusion pump (Alaris GP volumetric pump, Cardinal Health, Rolle, Switzerland). Baseline samples (MMIMS samples as described below, arterial and mixed venous blood samples, referred to as T2 hereafter) were taken 20 min after start of inert gas infusion, and vital parameters were recorded. After induction of lung damage and initial stabilization, samples were taken at 15-min intervals over a period of four hours to demonstrate the time course of the lung injury. Samples were labelled as T3 to T16 for every 15-min interval after lung injury.

2.3 Multiple inert gas elimination technique by micropore membrane inlet mass spectrometry

MIGET analysis has been described in previous studies [10, 11]. The inert gas infusion was prepared by removing the air from a 500 ml saline bag (four such bags were prepared) and adding 100 ml of sulphur hexafluoride (SF_6). The SF_6/saline mixture was shaken for 10 min to remove any dissolved air and the excess gas was expelled. 90 ml of pure SF_6 and 24 ml of pure krypton gas were added to the infusion bag. Finally, the following gases were added as liquid injections: 200 µl desflurane, 200 µl enflurane, 1 ml diethyl ether, and 5 ml acetone. The optimal individual inert gas concentrations were derived from preliminary MMIMS calibration experiments.

Blood samples for MIGET were collected simultaneously from the pulmonary artery and systemic artery catheters in gas-tight, ungreased, matched barrel glass syringes (Cadence Science Inc®, Plainfield Pike Cranston, RI, USA) with a three-way metal stopcock. After withdrawal of 5 ml of blood in a waste syringe to clear the dead space volume and to avoid air bubbles, 2.5–3 ml of blood was collected for the MMIMS method in 5 ml syringes prefilled with 0.2 ml concentrated EDTA. The syringes were sealed with a metal stopcock after a thorough inspection for any air bubbles. A mixed expired gas sample was collected in dry 50 ml matched barrel glass syringes from a heated (> 40 °C) mixing chamber (volume 2.5 l) connected to the ventilator outlet. Mixed expired sampling commenced, relative to the blood sampling, after 2.5 l of exhaled gas had passed through the mixing chamber. The collected samples were then subjected to inert gas partial pressure measurements using the MMIMS procedure as described in previous studies [9, 11]. All measurements where performed by a single investigator, who also prepared the gas syringes in between the measurements in this 15 min interval without further assistance.

Resultant retention and excretion data were transformed to V_A/Q distributions according to the data processing routines of the MMIMS-MIGET software (Version: 102312). Fractional MMIMS-derived shunt (shunt $\equiv V_A/Q < 0.005$) and MMIMS-derived dead space (dead space $\equiv V_A/Q > 100$) were determined as compartments of interest.

The iterative algorithm calculates the resulting retention and excretion values and generates a model V_A/Q distribution. The sum of squares of differences is then calculated for each gas by comparing the model calculated to that of the measured retention and excretion values. Then the algorithm alters the model V_A/Q distribution parameters, re-calculates the resulting retention and excretion values, and derives the new resulting sum of squares of differences. This process is repeated until no further reductions of the residual sum of squares can be achieved [17]. Residual sum of squares is reported with each V_A/Q distribution.

The Riley shunt and Bohr dead space fractions were calculated as previously reported [18–21].

2.4 Data analysis and statistics

Data were recorded with S5 collect (Datex-Ohmeda, Finland) and AcqKnowledge (Biopac Systems, Goleta, CA, USA). The R project software was used for statistical computing [22].

Normality analysis was performed using the Shapiro–Wilk test and optical interpretation of QQ plots for

each variable. Linear regression and a detailed Bland–Altman analysis [23, 24] were used to analyze the correlation and agreement between the methods. Variance analysis (ANOVA) was performed over the time course of shunt (MMIMS-derived shunt and Riley shunt) and dead space (MMIMS-derived dead space and Bohr dead space). Bonferroni corrections were made to account for repeated measurements.

The data were descriptively analyzed and the significance level (P value) for statistical tests was chosen as <0.05.

3 Results

Out of the 16 recruited pigs in the lavage group, 1 died and 15 remained. The pig died 30 min after lavage due to recurrent tension pneumothorax. In the pulmonary embolism group, out of the 14 recruited pigs, 4 were excluded and 10 remained. The exclusion was due to MMIMS deficiencies in instruments, handling, and equipment. Hence, a total of 25 pigs could be used for the statistical analysis.

The Shapiro–Wilk test for normality revealed P values <0.05 (data not normal) at 97% of time points for all variables, correlating well with the optical interpretation of QQ plots for each variable. The results are reported as medians and interquartile ranges. There were 15 pigs in the lavage group (median weight: 31 kg, IQR: 1.5 kg) and 10 pigs in the pulmonary embolism group (median weight: 30.25 kg, IQR: 4.37 kg). The hemodynamic and respiratory data are summarized Table 1, and the blood gas values in Table 2.

Figures 1, 2, 3 and 4 illustrate sample V*A*/Q distributions resulting from the MIGET by MMIMS method. For each model of injury, distributions at T2 (baseline, Figs. 1, 3) and after induction of lung damage (Figs. 2, 4) are depicted.

Table 1 Hemodynamic and respiratory data

	Baseline (T2)		Injury (T3)		End of experiment (T16)	
	Lavage (n = 15)	PE (= 10)	Lavage (n = 15)	PE (n = 10)	Lavage (n = 15)	PE (n = 10)
MAP (mmHg)	83 (12)	73 (17)	72 (14)	80 (29)	71 (13)	74 (4)
MPAP (mmHg)	12 (2)	13 (2)	19 (4)	30 (5)	19 (6)	23 (4)
HR (bpm)	100 (30)	103 (22)	88 (41)	120 (28)	110 (32)	106 (15)
CO (l/min)	4.5 (1.4)	4.7 (1.6)	3.8 (1.1)	3.8 (1.5)	5.2 (1.2)	4.2 (0.8)
MV (l/min)	5.9 (1.1)	6.1 (0.9)	6 (2)	6.7 (1.1)	7 (1.8)	7.4 (1.6)
Vt (ml)	246 (18)	254 (20)	257 (21)	254 (13)	248 (13)	256 (18)
PIP (mbar)	17 (2)	16 (2)	25 (3)	18 (3)	22 (1)	20 (4)
Pmaw (mbar)	8 (0)	8 (0)	10 (1)	8 (1)	10 (1)	8 (1)
$EtCO_2$ (mmHg)	38 (3)	37 (4)	37 (8)	30 (4)	32 (8)	30 (5)
Lung compliance	27.7 (3.9)	26.6 (4.4)	15.8 (1.7)	24.5 (5.6)	16.6 (2.5)	22.7 (5.1)

Hemodynamic and ventilation data for baseline, after injury and last measurement (T16). Median value (interquartile range)

MAP Mean arterial pressure, *MPAP* mean pulmonary arterial pressure, *HR* heart rate, *CO* cardiac output, *MV* minute ventilation, *Vt* tidal volume, *PIP* peak inspiratory pressure, *Pmaw* mean airway pressure, $EtCO_2$ end tidal carbon dioxide, *PE* pulmonary embolism

Table 2 Blood gas values

	Baseline (T2)		Injury (T3)		End of experiment (T16)	
	Lavage (n = 15)	PE (= 10)	Lavage (n = 15)	PE (n = 10)	Lavage (n = 15)	PE (n = 10)
$PaCO_2$ (mmHg)	39 (3)	41 (6)	48 (12)	52 (10)	48 (10)	46 (5)
$PvCO_2$ (mmHg)	49 (5)	49 (8)	56 (14)	62 (8)	57 (10)	60 (9)
PaO_2 (mmHg)	467 (74)	465 (34)	123 (74)	428 (83)	348 (48)	408 (77)
PvO_2 (mmHg)	50 (6)	48 (7)	43 (7)	51 (9)	55 (6)	52 (4)
SvO_2 (%)	72 (7)	71 (10)	57 (13)	68 (10)	72 (6)	72 (14)
Art Lact (mmol/l)	0.8 (0.5)	0.8 (0.3)	1.4 (2.2)	0.8 (0.6)	0.8 (0.2)	0.6 (0.2)
Hct (%)	27 (3.6)	24.3 (4.8)	26.7 (3)	27.1 (6.2)	24.8 (3.5)	23.2 (2.4)
PaO_2/FIO_2	472 (72)	470 (34)	124 (75)	432 (84)	413 (78)	356 (54)

Blood gas data for baseline, after injury and last measurement (T16). Median value (interquartile range)

PaCO$_2$ Arterial carbon dioxide tension, *PvCO*$_2$ mixed venous carbon dioxide tension, *paO*$_2$ arterial oxygen tension, *PvO*$_2$ mixed venous oxygen tension, *SvO*$_2$ mixed venous oxygen saturation, *Art Lact* arterial lactate, *Hct* hematocrit

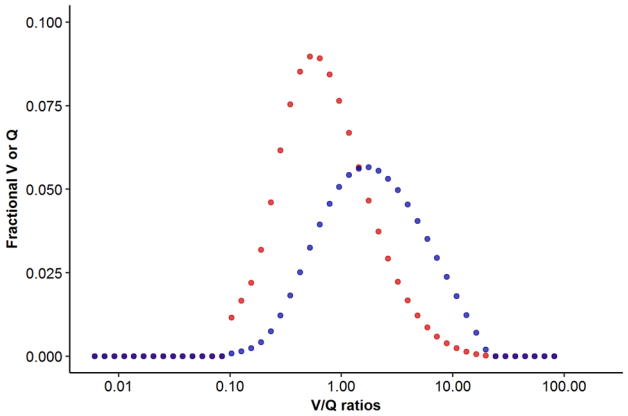

Fig. 1 V_A/Q distribution Pig 19 (lavage) at baseline (T2). MMIMS-derived dead space = 0.22, MMIMS-derived shunt = 0. Residual sum of squares = 8.5. V = ventilation (blue). Q = perfusion (red)

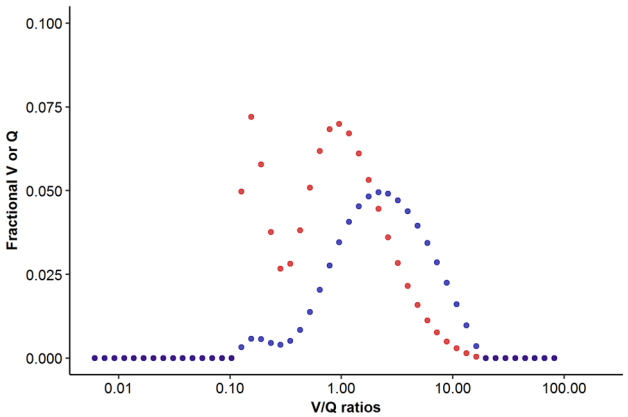

Fig. 2 V_A/Q distribution Pig 19 (lavage) after lung injury (T3). MMIMS-derived dead space = 0.39. MMIMS-derived shunt = 0.0826. Residual sum of squares = 8.8. V = ventilation (blue). Q = perfusion (red)

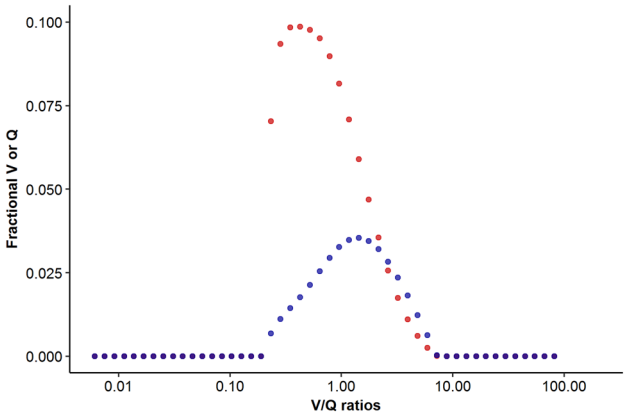

Fig. 3 V_A/Q distribution Pig 17 (pulmonary embolism) at baseline (T2). MMIMS-derived dead space = 0.62. MMIMS-derived shunt = 0. Residual sum of squares = 7.4. V = ventilation (blue). Q = perfusion (red)

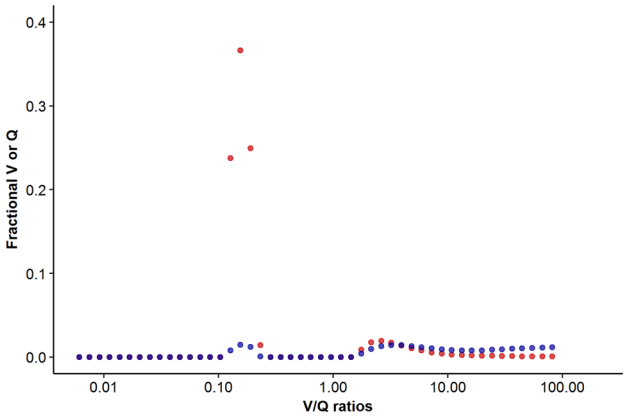

Fig. 4 V_A/Q distribution Pig 17 (pulmonary embolism) after lung injury (T3). MMIMS-derived dead space = 0.76. MMIMS-derived shunt = 0.013. Residual sum of squares = 5.2. V = ventilation (blue). Q = perfusion (red)

The analysis was based on 349 data pairs, comparing MMIMS-derived shunt to Riley shunt, and MMIMS-derived dead space to Bohr dead space. Fractional MMIMS-derived shunt and Riley shunt ranged from 0 to 0.36 and 0.04 to 0.58, respectively. Similarly, the range of fractional MMIMS-derived dead space and Bohr dead space was 0.23 to 0.58 and 0.47 to 0.89, respectively. Linear regression analyses are shown in Figs. 5 and 6. Both regression coefficients were statistically significant ($P < 0.0001$).

MMIMS-derived shunt was lower than Riley shunt on average (mean = −0.05, SD = 0.10 and bias = −0.06), with lower and upper limits of agreement of −0.15 and 0.04 (Fig. 7). In the case of dead space, MMIMS-derived dead space was lower than Bohr dead space on average (mean = −0.09, SD = 0.14 and bias = −0.09), with lower and upper limits of agreement of −0.24 and 0.05 (Fig. 8). As an indicator of experimental error, the MMIMS dataset had a residual sum of squares (RSS) < 5.3 in 27.8%, RSS < 10.6 in 51.3% and RSS < 16.8 in 63%.

MMIMS-derived shunt (Fig. 9) increased in the lavage group, and MMIMS-derived dead space (Fig. 10) increased in both groups after the induction of lung damage (dashed line). ANOVA revealed significant differences in MMIMS-derived shunt between the injury models as well as for the time course after lung injury. MMIMS-derived dead space differed significantly for the time course after lung injury, but not between the injury models. Bohr-derived dead space also showed no significant differences between injury models.

In acute lung injury caused by lavage, we saw a rapid recovery in the first 150 min after lavage, indicated by the

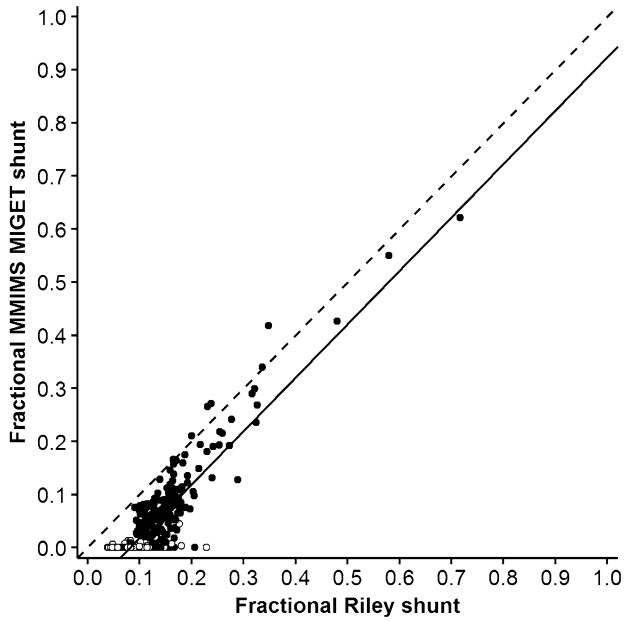

Fig. 5 Linear regression of MMIMS-derived shunt on Riley shunt. Closed circles = lavage (LAV). Open circles = pulmonary embolism (PE). MMIMS-derived shunt = −0.081 + 1.006 * Riley shunt, $R^2 = 0.788$. $P < 0.0001$. Dashed line = line of identity. Solid line = regression line

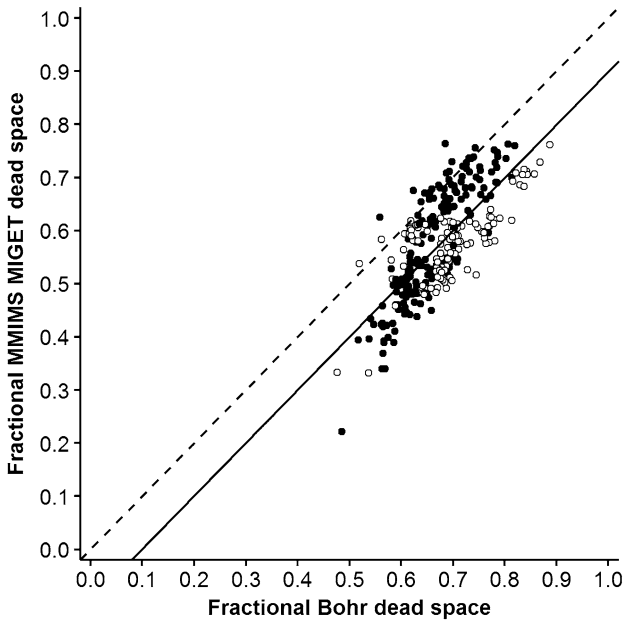

Fig. 6 Linear regression for MMIMS-derived dead space on Bohr dead space. Closed circles: lavage (LAV). Open circles = pulmonary embolism (PE). MMIMS-derived dead space = −0.099 + 0.998 * Bohr dead space, $R^2 = 0.56$. $P < 0.0001$. Dashed line = line of identity. Solid line = regression line

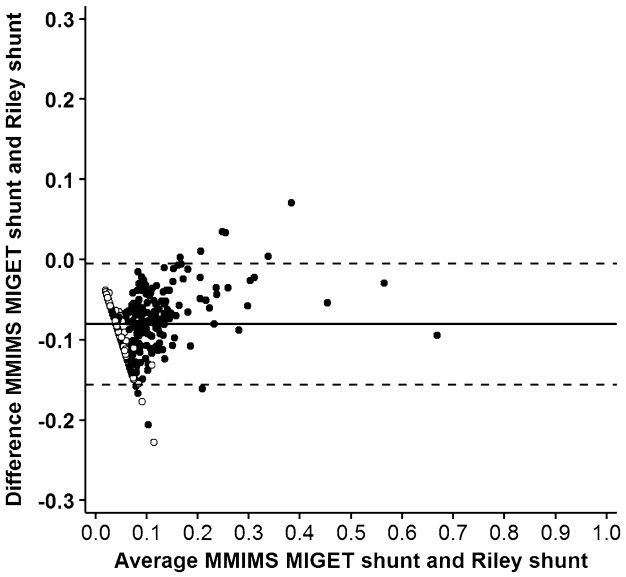

Fig. 7 Bland–Altman analysis of MMIMS-derived shunt and Riley shunt. Closed circles = lavage (LAV). Open circles = pulmonary embolism (PE). Mean (bias) ± 2*SD = −0.8 ± 0.076. Solid line = mean (bias). Dashed line = upper and lower limits of agreement

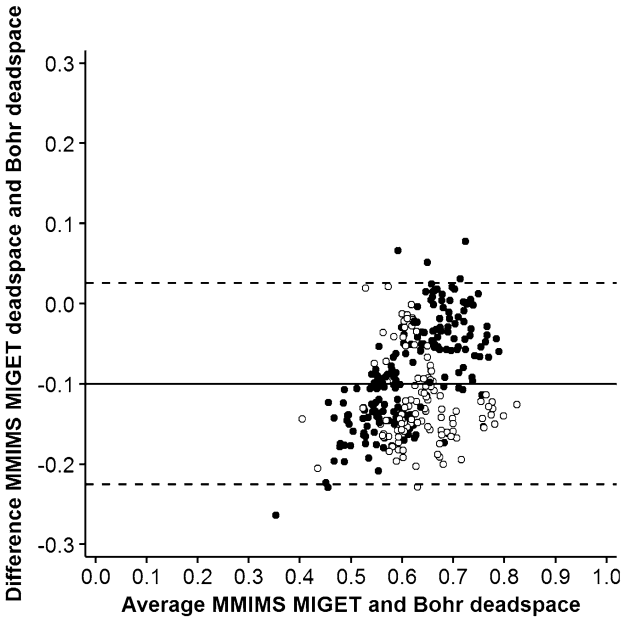

Fig. 8 Bland Altmann diagram of MMIMS-derived dead space and Bohr dead space. Closed circles = lavage (LAV). Open circles = pulmonary embolism (PE). Mean (bias) ± 2*SD = −0.1 ± 0.125. Solid line = mean (bias). Dashed line = upper and lower limits of agreement

MMIMS-derived shunt (Fig. 9). In contrast, the MMIMS-derived deadspace showed no recovery over this time period (Fig. 10).

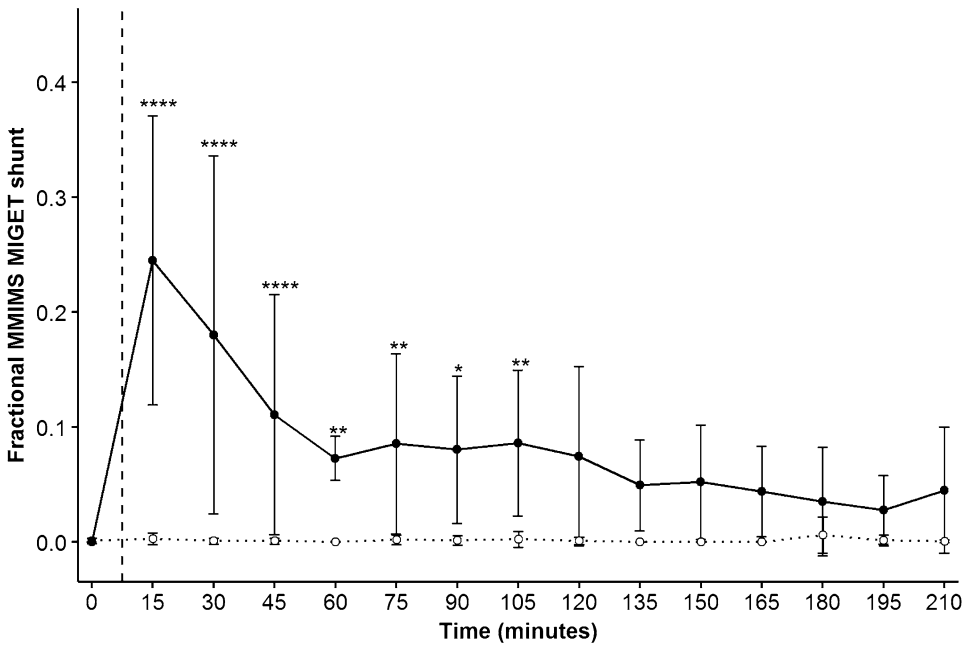

Fig. 9 Time course of MMIMS-derived shunt. Closed circles = lavage (LAV). Open circles = pulmonary embolism (PE). BL = baseline. Dashed line = time of injury. Parameters are indicated as mean and standard deviation. *P < 0.0033, **P < 0.0006, ***P < 0.00006, ****P < 0.000006. ANOVA Damage: P = 8e−05, ANOVA Time: P = 0e + 0, ANOVA Damage*Time: P = 1e−16

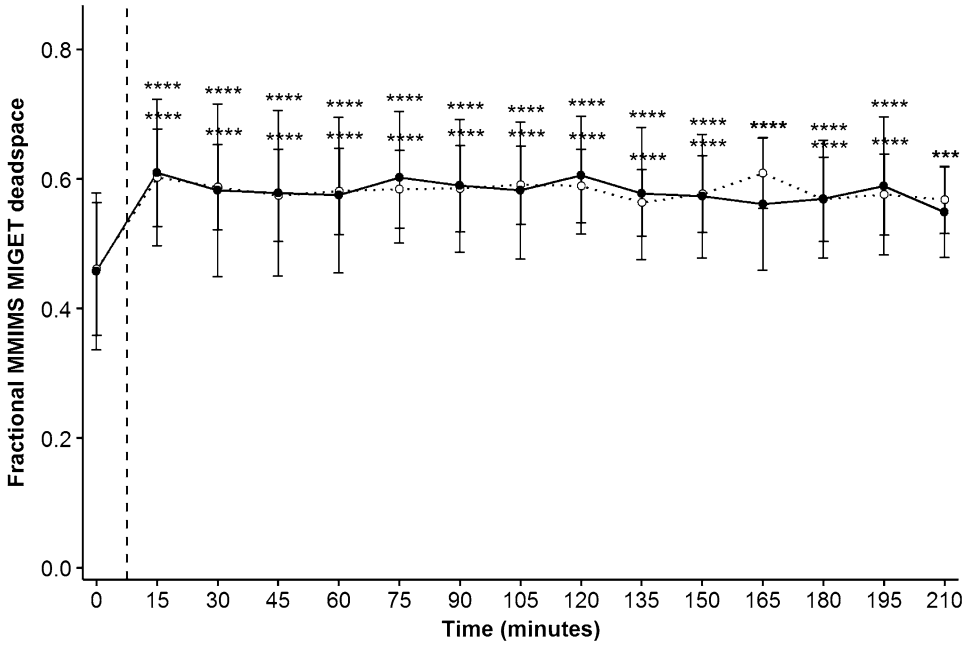

Fig. 10 Time course of MMIMS-derived dead space. Closed circles = lavage (LAV). Open circles = pulmonary embolism (PE). BL = baseline. Dashed line = time of injury. Parameters are indicated as mean and standard deviation. *P < 0.005, **P < 0.001, ***P < 0.0001, ****P < 0.0000. ANOVA Damage: P = 8e−01, ANOVA Time: P = 0e+0, ANOVA Damage*Time: P = 1e+00

4 Discussion

This work demonstrates for the first time that the MMIMS-MIGET method can feasibly measure shunt and deadspace at a high time resolution of 15-min intervals. MMIMS-derived shunt correlates ($R^2 = 0.788$) and agrees (lower and upper limits of agreement of −0.15 and 0.04) with Riley shunt. Similarly, MMIMS-derived dead space correlates ($R^2 = 0.56$) and agrees (lower and upper limits of agreement of −0.24 and 0.05) with Bohr dead space. MMIMS-derived shunt increased significantly after lung injury only in the lavage group, whereas MMIMS-derived dead space increased significantly in both groups.

MMIMS-MIGET-based analysis of V*A*/Q matching confirmed the well-described pattern of massive initial shunt increase with gradual decrease after induced lavage lung injury, but not after autologous clot pulmonary embolism (Fig. 9). Both injury models resulted in a moderate increase in MMIMS-derived dead space and Bohr dead space which persisted over the observed time period of 4 h (Fig. 10; Table 2). Our data on lavage injury and pulmonary

embolism are consistent with previous work using conventional MIGET. Dead space in the range of 50% already at baseline seems to be representative for pigs, as our measurements are in the same range reported by other groups with MIGET [25, 26] or Bohr dead space and volumetric capnography [13, 21] in pigs.

A factor contributing to the high dead space measurements could be the dilution of the inert gases—especially the soluble ones—in the ventilator circuit and mixing box for gas sampling with a total volume of 4.24 l. In addition, there is evidence of relevant inert gas exchange over, and accumulation in, the mucus of the airways, especially for highly blood-soluble gases [27, 28]. This might lower the excretion of acetone and diethyl ether, resulting in high MMIMS-derived dead space results. Higher lung water content after lavage explains the increase in measured dead space after lavage.

Whilst Neumann et al. [14] observed a 45% increase in shunt and a 14% increase in dead-space in a porcine model with induced lavage injury, Wagner et al. observed a significant increase in compartments with a V*A*/Q of > 10 in dogs, but no increase in dead space [29]. Our measurements of dead space were not discriminative for the model of injury. With the already high baseline dead space fractions of 50–60% measured in our study, induction of additional dead space is limited by the physiologic requirement for sufficient gas exchange. Differences in animal models and methods used to induce acute pulmonary embolism may explain minor discrepancies in findings.

After acute lung injury by lavage, recruitment of shunted alveoli started. The 15-min measurement interval allowed detailed observation of the time course. There is marked recovery in the first 60 min after lung injury, with the speed of recovery declining afterwards.

For dead space, no such recovery can be seen, which seems reasonable from a pathophysiological point of view.

The negative offset of MMIMS-derived shunt compared to Riley shunt has already been described by Duenges et al. [10], who reported an intercept of—4.3 and a slope of 0.60. Our values (intercept − 0.08, slope 1.003, r 0.88) show a closer correlation, which may be explained by the refinements of the MMIMS system (multi-pore inlet) compared to the study of Duenges with the single-pore inlet of a mass spectrometer. For conventional gas chromatography (GC) MIGET methods, Wagner [29] reported an intercept of − 1.29, a slope of 1.02 and r of 0.96 (with inverted GC-MIGET and Riley shunt axis to facilitate comparison).

MMIMS-MIGET assesses solely intrapulmonary shunt. This is in contrast to Riley shunt, which lumps together intrapulmonary and extrapulmonary shunt [29] and very low V*A*/Q, partly explaining why MMIMS-derived shunt fraction was lower than Riley shunt on average. In addition, the underestimation increases proportionally with the increasing low V*A*/Q component of the higher shunt levels. Further study is required to determine whether systematic negative offsets reflect superior resolution by MMIMS-MIGET at the extremes of V*A*/Q distribution.

One limitation of all MIGETmethods is the need for mixed-venous samples and thus for a pulmonary catheter in place. The possibility of replacing the mixed venous sample with a sample that is more widely available (e.g., a central venous or peripheral venous sampling site) has to be evaluated in further studies.

Another limitation of all MIGET methods is the need for inert gas infusion, which may result in relevant amounts of additional fluids. In our protocol, we used infusion rates of about 7–10 ml/kg/h. Infusion rates as low as 1/1000th of baseline cardiac output were suggested by the MMIMS manufacturer, but yielded unacceptable signal-to-noise ratios.

The mathematic model behind the MIGET methods requires a steady-state situation. Although the MIGET by MMIMS measurement method is fast enough to provide results even during the dynamically changing situations in an operating room, one should always consider whether the samples were taken in a steady-state situation. Furthermore, a statistical limitation of our study is the usage of ANOVA test for consecutive measurements, although the underlying data is not normal. Since the analysis involved was purely descriptive in nature, and no confirmatory statistical outcomes are being claimed, ANOVA test seems to be the best of the available options for two-way repeated measurements.

In summary, this work demonstrates good correlation between, and agreement of fractional shunt and dead space, between MIGET by MMIMS and conventional respiratory gas analysis. MIGET by MMIMS is the first application that returns clinically relevant results in due time for therapeutic action and subsequent monitoring. This work demonstrates the feasibility of V*A*/Q measurements with a 15-min time resolution in a large animal model with two injury models, and would allow for further study of therapeutic interventions in an animal model.

Acknowledgements The authors thank Daniel Mettler and Olgica Beslac of the ESI, Experimental Surgery Unit, medical faculty of the University of Bern, Switzerland, for providing the infrastructure and very helpful support and assistance. We would also like to thank Lukas Häller, Master's Student in Medicine at the University of Bern, for assistance with data acquisition, sample collection, handling and transport. The authors thank Jeannie Wurz for her proofreading and English language editing support. This research was supported by SNF Grant 320030_133046.

Compliance with ethical standards

Conflict of interest The authors declare that they have no conflicts of interest.

Ethical approval All procedures performed in studies involving animals were in accordance with the ethical standards of the cantonal ethics committee of Bern, Switzerland.

References

1. Hedenstierna G, Edmark L. The effects of anesthesia and muscle paralysis on the respiratory system. Intensive Care Med. 2005;31(10):1327–35. https://doi.org/10.1007/s00134-005-2761-7.
2. Powell ES, Pearce AC, Cook D, Davies P, Bishay E, Bowler GM, Gao F, Co-ordinators U. UK pneumonectomy outcome study (UKPOS): a prospective observational study of pneumonectomy outcome. J Cardiothorac Surg. 2009;4:41. https://doi.org/10.1186/1749-8090-4-41.
3. Zambon M, Vincent JL. Mortality rates for patients with acute lung injury/ARDS have decreased over time. Chest. 2008;133(5):1120–7. https://doi.org/10.1378/chest.07-2134.
4. Riley RL, Cournand A, Donald KW. Analysis of factors affecting partial pressures of oxygen and carbon dioxide in gas and blood of lungs; methods. J Appl Physiol. 1951;4(2):102–20.
5. Wagner PD. The multiple inert gas elimination technique (MIGET). Intensive Care Med. 2008;34(6):994–1001. https://doi.org/10.1007/s00134-008-1108-6.
6. Sapsford DJ, Jones JG. The PIO2 vs. SpO2 diagram: a non-invasive measure of pulmonary oxygen exchange. Eur J Anaesthesiol. 1995;12(4):375–86.
7. Thomsen LP, Karbing DS, Smith BW, Murley D, Weinreich UM, Kjærgaard S, Toft E, Thorgaard P, Andreassen S, Rees SE. Clinical refinement of the automatic lung parameter estimator (ALPE). J Clin Monit Comput. 2013;27(3):341–50. https://doi.org/10.1007/s10877-013-9442-9.
8. Wagner PD, Dantzker DR, Dueck R, Clausen JL, West JB. Ventilation-perfusion inequality in chronic obstructive pulmonary disease. J Clin Investig. 1977;59(2):203–16. https://doi.org/10.1172/JCI108630.
9. Baumgardner JE, Choi IC, Vonk-Noordegraaf A, Frasch HF, Neufeld GR, Marshall BE. Sequential V(A)/Q distributions in the normal rabbit by micropore membrane inlet mass spectrometry. J Appl Physiol. 2000;(1985) 89(5):1699–708.
10. Duenges B, Vogt A, Bodenstein M, Wang H, Bohme S, Rohrig B, Baumgardner JE, Markstaller K. A comparison of micropore membrane inlet mass spectrometry-derived pulmonary shunt measurement with Riley shunt in a porcine model. Anesth Analg. 2009;109(6):1831–5. https://doi.org/10.1213/ANE.0b013e3181bbc401.
11. Kretzschmar M, Schilling T, Vogt A, Rothen HU, Borges JB, Hachenberg T, Larsson A, Baumgardner JE, Hedenstierna G. Multiple inert gas elimination technique by micropore membrane inlet mass spectrometry—a comparison with reference gas chromatography. J Appl Physiol. 2013;(1985) 115(8):1107–18. https://doi.org/10.1152/japplphysiol.00072.2013.
12. Hlastala MP, Colley PS, Cheney FW. Pulmonary shunt: a comparison between oxygen and inert gas infusion methods. J Appl Physiol. 1975;39(6):1048–51.
13. Tusman G, Sipmann FS, Borges JB, Hedenstierna G, Bohm SH. Validation of Bohr dead space measured by volumetric capnography. Intensive Care Med. 2011;37(5):870–4. https://doi.org/10.1007/s00134-011-2164-x.
14. Neumann P, Hedenstierna G. Ventilation-perfusion distributions in different porcine lung injury models. Acta Anaesthesiol Scand. 2001;45(1):78–86.
15. Rees SE, Kjaergaard S, Andreassen S, Hedenstierna G. Reproduction of MIGET retention and excretion data using a simple mathematical model of gas exchange in lung damage caused by oleic acid infusion. J Appl Physiol (1985). 2006;101(3):826–32. https://doi.org/10.1152/japplphysiol.01481.2005.
16. Kjaergaard B, Kristensen SR, Risom M, Larsson A. A porcine model of massive, totally occlusive, pulmonary embolism. Thromb Res. 2009;124(2):226–9. https://doi.org/10.1016/j.thromres.2009.01.010.
17. Wagner PD, Saltzman HA, West JB. Measurement of continuous distributions of ventilation-perfusion ratios: theory. J Appl Physiol. 1974;36(5):588–99.
18. Riley RL, Cournand A. Ideal alveolar air and the analysis of ventilation-perfusion relationships in the lungs. J Appl Physiol. 1949;1(12):825–47.
19. Bohr C. Über die Lungenatmung. Skand Arch Physiol. 1891;2:236–8.
20. Fowler WS. Lung function studies; the respiratory dead space. Am J Physiol. 1948;154(3):405–16.
21. Tusman G, Sipmann FS, Bohm SH. Rationale of dead space measurement by volumetric capnography. Anesth Analg. 2012;114(4):866–74. https://doi.org/10.1213/ANE.0b013e318247f6cc.
22. Team RC. (2016) R: a language and environment for statistical computing. R Foundation for Statistical Computing, Vienna. 2015. http://www.R-projectorg.
23. Bland JM, Altman DG. Statistical methods for assessing agreement between two methods of clinical measurement. Lancet. 1986;1(8476):307–10.
24. Bland JM, Altman DG. Measuring agreement in method comparison studies. Stat Methods Med Res. 1999;8(2):135–60.
25. Kretzschmar M, Kozian A, Baumgardner JE, Schreiber J, Hedenstierna G, Larsson A, Hachenberg T, Schilling T. Bronchoconstriction induced by inhaled methacholine delays desflurane uptake and elimination in a piglet model. Respir Physiol Neurobiol. 2016;220:88–94. https://doi.org/10.1016/j.resp.2015.09.014.
26. Batchinsky AI, Weiss WB, Jordan BS, Dick EJ Jr, Cancelada DA, Cancio LC. Ventilation-perfusion relationships following experimental pulmonary contusion. J Appl Physiol (1985). 2007;103(3):895–902. https://doi.org/10.1152/japplphysiol.00563.2006.
27. George SC, Babb AL, Hlastala MP. Dynamics of soluble gas exchange in the airways. III. Single-exhalation breathing maneuver. J Appl Physiol (1985). 1993;75(6):2439–49.
28. Anderson JC, Hlastala MP. Impact of airway gas exchange on the multiple inert gas elimination technique: theory. Ann Biomed Eng. 2010;38(3):1017–30.
29. Wagner PD, Laravuso RB, Goldzimmer E, Naumann PF, West JB. Distribution of ventilation-perfusion ratios in dogs with normal and abnormal lungs. J Appl Physiol. 1975;38(6):1099–109.